

SOLIDIFICATION OF BORATE ION-EXCHANGE RESINS BY ALKALI-ACTIVATED SLAG CEMENTS

NAILIA R. RAKHIMOVA¹ *, RAVIL Z. RAKHIMOV², YEVGEN S. LUTSKIN³,
VLADIMIR P. MOROZOV⁴, YURI N. OSIN⁴

¹Faculty of Civil Engineering, Ton Duc Thang University (Ho Chi Minh City, Vietnam)

²Kazan State University of Architecture and Engineering (Kazan, Russian Federation)

³Odessa State Academy of Civil Engineering and Architecture (Odessa, Ukraine)

⁴Kazan Federal University (Kazan, Russian Federation)

In this study, a mineral matrix based on alkali-activated slag cement (AASC) was found to be suitable for solidification of up to 35% (by volume) of borate ion-exchange resins (IERs) at pH values of 8.5 to 10.5. Experimental-statistical modelling, X-ray diffraction, and scanning electron microscopy/energy dispersive spectroscopy analyses were used to study the waste samples. According to the results of a four-factor experiment, the strengths of waste samples based on AASC-based mineral matrices and borate IERs were mostly determined by the nature of the alkali component and the pH of the borate IERs. The strengths of the waste samples could be improved by some modifications of the binder material - increasing the Na₂O concentration and introducing polypropylene fibres. The main reaction products in the (GGBFS)-(sodium metasilicate, sodium hydroxide)-(borate solution) system were C-(A)-S-H, calcite (CaCO₃), hydrotalcite (Mg_{0.667}Al_{0.333}(OH)₂(CO₃)_{0.167}(H₂O)_{0.5}, calcium silicate hydrates C-S-H (I) - CaO·SiO₂·H₂O and Ca_{1.5}SiO_{3.5}·H₂O, and ulexite NaCaB₅O₆(OH)₆(H₂O)₅.

Keywords: alkali-activated slag cement, modeling, ion-exchange resin waste, compressive strengths, calorimetric test, polypropylene fibre

1. Introduction

Improving materials and approaches for the reliable immobilization of radioactive waste while addressing rising environmental safety requirements is important to the development of nuclear power engineering. Ion exchange resins (IERs) are a common type of wet radioactive waste. IERs are used widely within the nuclear industry to decontaminate radioactive effluents. The spent resins must be stabilized and solidified into a solid, stable, monolithic and confining form [1]. IERs which represent low or intermediate level radioactive wastes are usually embedded before being stored in different encapsulation materials such as organic resins (epoxy) or cement-based materials. The procedure for immobilization of IERs into cement is simple. However, the final waste volume affects the cost of transportation and disposal. Thus, future research on cement immobilization should focus on reducing porosity, optimizing cement and additive types to increase resin loading, enhancing compressive strength, and reducing the nuclide leach rate [2].

The IER content in Portland cement solidification products should be maintained below 20% [3]. IERs are highly porous materials with poor mechanical strength. The higher their content in the matrix, the lower the compressive strength of the

resulting material [4]. In addition, spent IERs contain radionuclides and chemical species which are present in the treated waste streams (for instance, borate and lithium ions in IERs used to purify the primary circuits of pressurized water reactors, or sodium and nitrate ions in IERs used to purify solutions produced during spent fuel reprocessing). The concentrations of chemical species can be high and compatibility with Portland cement-based mineral matrix is limited. It reported that the boric acid content which is present in spent anion resins from pressurized water reactor power stations in the spent resin from PWR is 50 to 70g/kg leads to delay of the hardening process of ordinary Portland cement, poor product stability, and lower waste stabilization in the product [5]. Hence, inclusion of reinforcing materials (such as stainless steel, fiber glass, and carbon fibres) and stronger mineral matrices including alkali-activated slag cement (AASC)-based cementitious materials are being considered as ways to improve the properties of borate-containing cemented IERs [6-13].

In this study, the feasibility of solidification of simulated radioactive borate IERs with sodium metasilicate and hydroxide AASC was investigated. The microstructures of the hardened matrices and properties of the fresh and hardened pastes and hydration products were studied. The quantity and nature of the alkali activator, concentration of

* Autor corespondent/Corresponding author,
E-mail: nailia.rakhimova@tdt.edu.vn

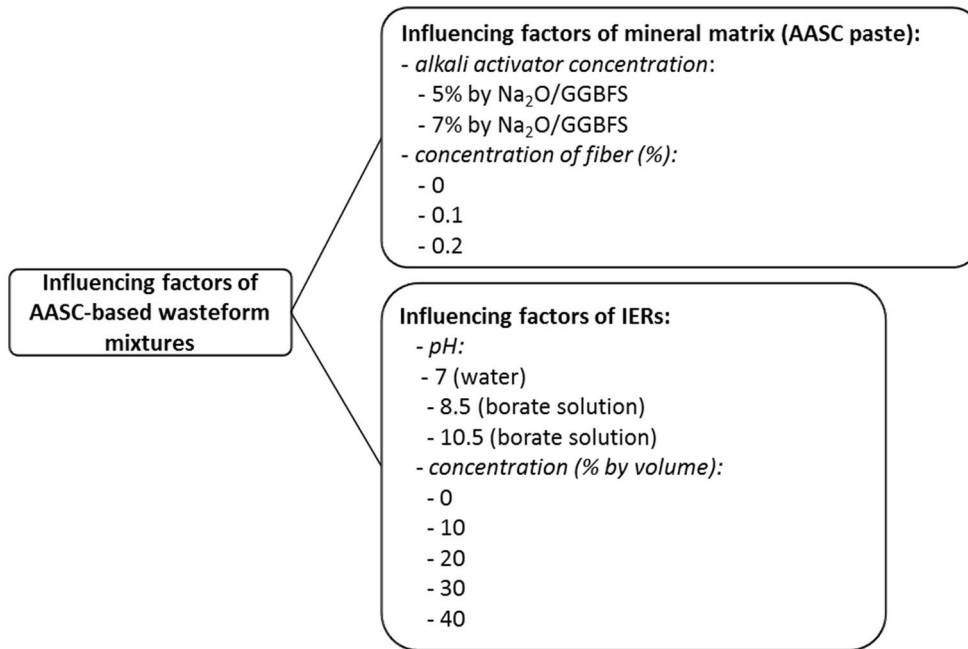


Fig. 1 - Influencing factors of the waste samples based on AASC-based mineral matrices and borate IERs.

Table 1

Chemical composition of GBFS												
Component (mass % as oxide)												
SiO ₂	CaO	Al ₂ O ₃	MgO	MnO	Fe ₂ O ₃	TiO ₂	Na ₂ O	K ₂ O	P ₂ O ₅	SO ₃	CO ₂	LOI
37.49	36.22	11.58	8.61	0.50	0.16	1.80	0.64	0.95	0.01	2.00	-	-

polypropylene fibre, and pH and concentrations of the IERs were considered as variables. The dependence of the main properties of the binding material on the factors is listed in Figure 1 was examined in detail.

2. Experimental details

Granulated blast furnace slag (GBFS) obtained from the Magnitogorsky factory was ground in a laboratory planetary mill to a specific surface area (S_{sp}) of 300 m²/kg (Blaine). The chemical and mineralogical compositions of GBFS are shown in Table 1 and Figure 2, respectively. X-ray analysis of GBFS shows that it consists primarily of an amorphous phase with small amounts of gehlenite $Ca_2Al_2SiO_7$, calcite, akermanite $Ca_2(Mg_{0.75}Al_{0.25})(Si_{1.75}Al_{0.25}O_7)$, hatrurite $Ca_3(SiO)_4$, and stebroorskite $Ca_2Fe_2O_5$.

The alkali activation of the GBFS was carried out using commercial sodium metasilicate hydrate $Na_2SiO_3 \cdot 9H_2O$ (NSH₉) and sodium hydroxide (NaOH). The dosage of alkali components were used to obtain the Na₂O content of 5-7% reported to slag.

To simulate borate IERs, cationic IERs were saturated in 200 g/l of borate solutions of pH 8.5 and 10 (Table 2). IERs were supplied by “Azot” (Cherkassy, Ukraine) under the trade name KU-2-8 in the physical form of spherical beads or ground grains. They had diameters of 0.35 - 0.55 μm. Borate solutions designed to simulate real borate

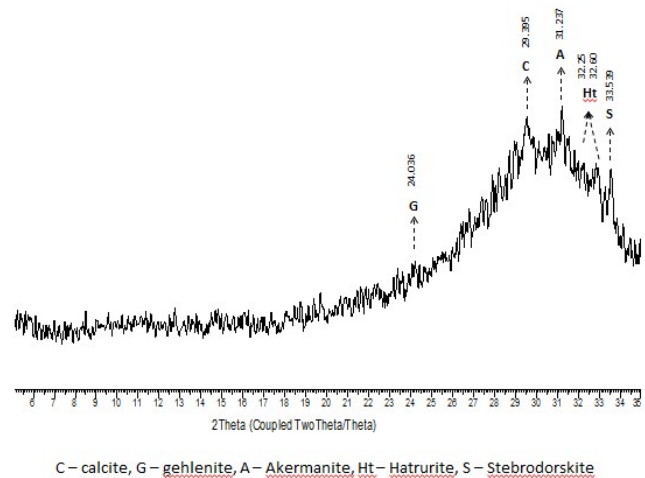


Fig. 2 - X-ray diffractogram of GBFS.

radioactive liquid waste produced in a nuclear power plant's pressurized water reactor were prepared by dissolving H₃BO₃ and NaOH in tap water. A control sample was prepared using an equal volume of sodium hydroxide solution and sodium metasilicate solution.

Cementitious waste samples were prepared by mixing the wet saturated borate IERs with a dry mix of GGBFS and NSH₉ or NaOH. A liquid/solid ratio of 0.45 provided a workable and appropriate fresh paste flowability.

As reinforcing material commercial (EuroCHEM) polypropylene fibre with length 3 mm

Table 2

Composition of prepared simulated borate solutions				
Borate solution	Concentration of NaOH(mol/l)	Concentration of H ₃ BO ₃ (mol/l)	Concentration of simulated borate solution(g/l)	pH
Borate solution 1	2.670	0.830	200	8.5
Borate solution 2	2.670	0.420	200	10.5

was used.

The AASC paste samples were prepared in cubic moulds (4 × 4 × 4 cm) for compressive strength test, after 1 day of curing under normal conditions (room temperature, humidity 95-100%) and then were demoulded. The cubes were stored in sealed plastic bags in a chamber at room temperature and 95-100% relative humidity, for 28 days. Each strength determination reported is based on the average of six measurements for the same cast.

Calorimetry experiments were carried out using “Thermochron” metering equipment. The pastes were mixed externally, placed in sealed glass ampoules, and loaded into the calorimeter. The time elapsed between the addition of the activator and water or saturated borate IERs to the powder and the loading of the paste into the calorimeter was approximately 3 - 4 min. The tests were run for 96 h.

X-ray diffraction (XRD) was performed on crushed GBFS and AASC paste samples that had been hardened for 28 days. In order to accelerate interaction of AASC paste and borate salts the samples for XRD have been prepared of GGBFS having S_{sp} 800 m²/kg. XRD data were collected using a D2 Phaser X-ray diffractometer in a Bragg-Brentano θ - 2θ configuration with Cu K α radiation, operating at 40 kV and 30 mA. The data handling was performed using the DIFFRACplus Evaluation Package – EVA Search/Match and database PDF-2 ICDD.

The preparation of fragments of selected samples after 28 days of curing for scanning electron microscopy (SEM, Merlin of CARL ZEISS) observations was done by embedding in epoxy resin, polishing, and carbon coating (Figure 3). For qualitative analysis, a set of etalons established in the program Aztec was used (reference standards for X-RAY microanalysis ‘Registered Standard No. 8842’).



Fig. 3 - The samples for scanning electron microscopy.

Design of experiment was performed using COMPEX software [14-16].

3. Results and discussion

3.1. Properties of fresh AASC pastes

The results of the calorimetric studies are shown in Figure 4. Increasing the pH of the borate IERs reduces the intensities and temperatures of the peaks, while also broadening them.

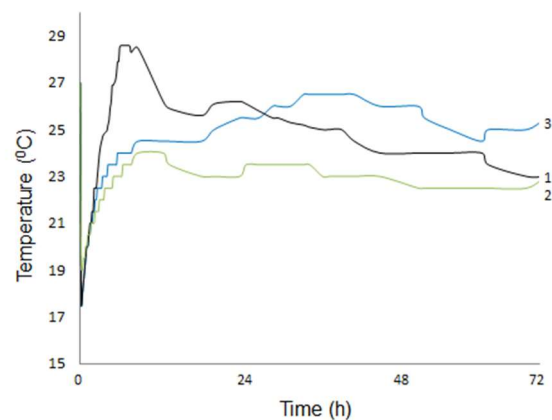


Fig. 4 - The hydration rates of fresh AASC pastes containing 20% of IERs at pH 7 (1), borate IERs at pH 8.5 (2), and borate IERs at pH 10.5 (3).

3.2. Properties of hardened AASC pastes

Table 3 shows the 28-day compressive strengths of hardened AASC pastes and analysis of the compressive strength and influencing factors based on serial regression analysis with generated error of experiment.

Experimental-statistical models of the factors influencing the 28-day compressive strengths follow:

for sodium hydroxide-activated waste samples:

$$R = 6.915 + 1.288x_1 - 14.824x_2 + 0.641x_3 + 0.132x_4 - 1.020x_1x_2 + 0.188x_1x_3 - 0.072x_1x_4 - 0.753x_2x_3 - 0.148x_2x_4 + 0.169x_3x_4 + 0.546x_1^2 + 9.409x_2^2 - 1.305x_3^2 + 0.621x_4^2$$

for sodium metasilicate-activated waste samples:

$$R = 9.657 + 3.130x_1 - 22.120x_2 - 1.040x_3 + 0.842x_4 - 2.495x_1x_2 + 0.385x_1x_3 - 0.158x_1x_4 - 0.556x_2x_3 - 0.985x_2x_4 + 0.083x_3x_4 + 0.550x_1^2 + 13.847x_2^2 + 5.510x_3^2 + 0.691x_4^2$$

Table 3

28-day compressive strengths of hardened AASC pastes and ranges of variation of normal and coded influencing factors

Run no.	Factors												Compressive strength (MPa)	
	X ₁			X ₂			X ₃			X ₄			Alkali activator	
	-1	0	1	-1	0	1	-1	0	1	-1	0	1	Sodium hydroxide	Sodium metasilicate
	Concentration of Na ₂ O (%)			Concentration of IERs (% by volume)			pH of IERs			Concentration of fiber (%)				
1..16	5...7			0...40			7...10.5			0...0.2			30...2.3	49...9.9
17...32	5			0...40			7 (water)			0...0.2			26...0	41...4.1
33..48							8.5 (borate solution)						28..0	44..5.6
49..64							10.5 (borate solution)						36...3.1	56.8...10
65...80	7			0...40			7 (water)			0...0.2			32...2.6	49.7...4.3
81...96							8.5 (borate solution)						34...2.7	56.2...7.3
							10.5 (borate solution)							

Analysis of the results presented in Figures 5-7 shows that the 28-day compressive strengths of AASC waste samples increase with

- increasing the Na₂O concentration and
- introducing polypropylene fibres,

and decrease with

- increasing the IER concentration,
- including borate-saturated IERs, and
- decreasing the pH of borate IERs.

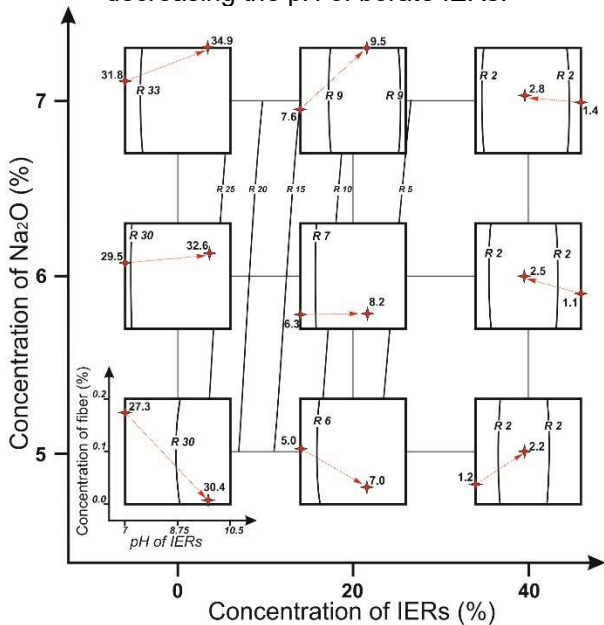


Fig.5 - 28-day compressive strengths of hardened AASC pastes containing IERs and activated by sodium hydroxide, as functions of various influencing factors.

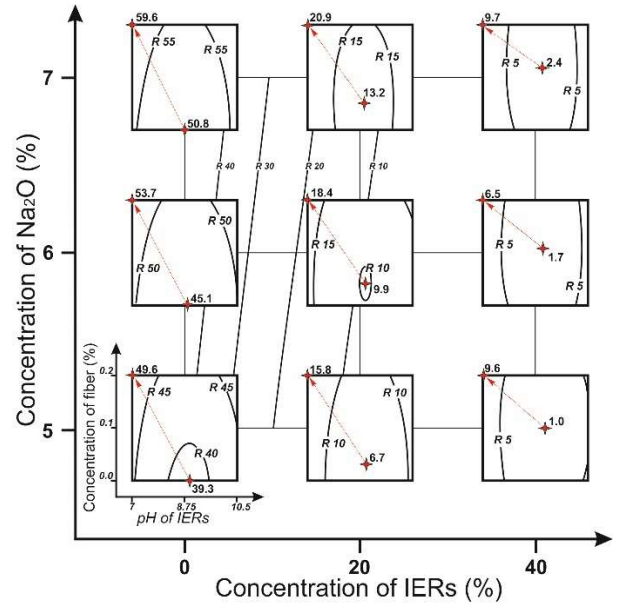
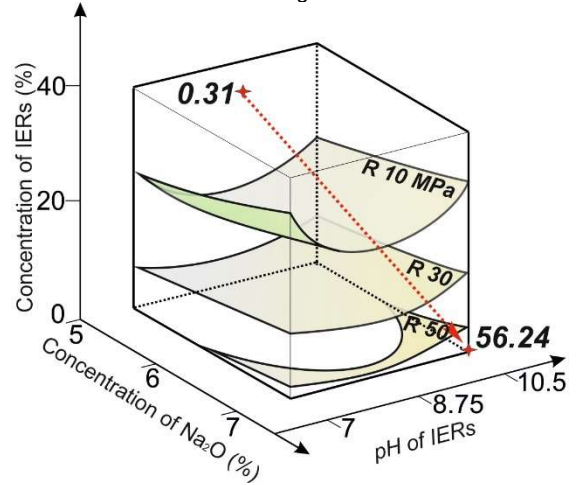
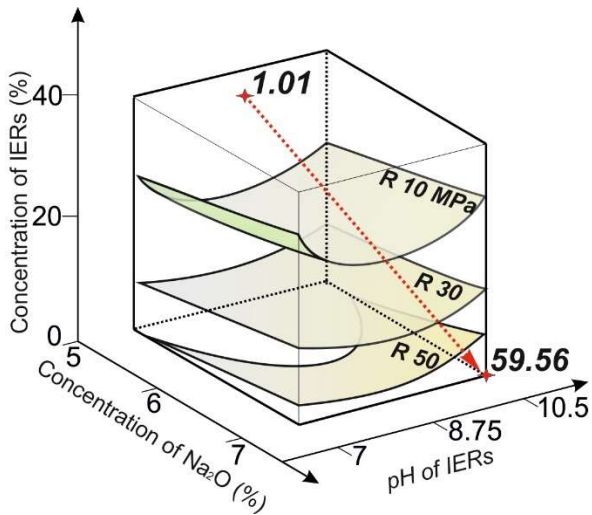


Fig.6 - 28-day compressive strengths of hardened AASC pastes containing IERs and activated by sodium metasilicate, as functions of on influencing factors.



a) Fig. 7 continues on next page



b)
Fig.7 - 28-day compressive strengths of hardened AASC pastes containing IERs and activated by sodium metasilicate, as functions of on influencing factors: (a) without polypropylene fibres, (b) with 0.2% polypropylene fibres

Sodium metasilicate-activated AASC waste samples demonstrate higher 28-day compressive strengths and IERs loads than sodium hydroxide-activated waste samples.

Regulatory requirements for compressive strengths of cementitious waste samples in various countries are follows: 0.35 MPa in France, 3.4 MPa

in the United States, 5 MPa in Slovakia, 7 MPa in the UK, 5 MPa in Russian Federation, and 10 MPa in Switzerland [17]. The compressive strengths of sodium hydroxide (7% Na₂O) AASC waste samples (9-9.5 MPa) nearly meet the most stringent requirements with borate IER content of 20%. This is the same as for Portland cement based waste samples incorporated with borate IERs. Sodium metasilicate AASC waste samples with borate IERs content of 35% exhibit compressive strengths of 9.4-13 MPa, depending on the borate IERs pH.

3.3. The influence of borate solutions on the composition of the hydration products and on the microstructure of hardened AASC pastes

3.3.1. X-ray diffraction

The results of XRD analysis are shown in Figures 8 and 9. The main reaction products in the GGBFS- sodium hydroxide (metasilicate)-borate system are: C-(A)-S-H (broad hump), calcite (CaCO₃) (reflection at 2θ = 29.395), hydrotalcite (MgO_{6.667}Al_{0.333})(OH)₂(CO₃)_{0.167}(H₂O)_{0.5} (reflection at 2θ = 11.649), calcium silicate hydrate C-S-H (I) - CaO-SiO₂-H₂O (reflection at 2θ = 7.066), calcium silicate hydrate C-S-H Ca_{1.5}SiO_{3.5}H₂O (reflection at 2θ = 29.356), and ulexite NaCaB₅O₆(OH)₆(H₂O)₅ (reflection at 2θ = 7.14).

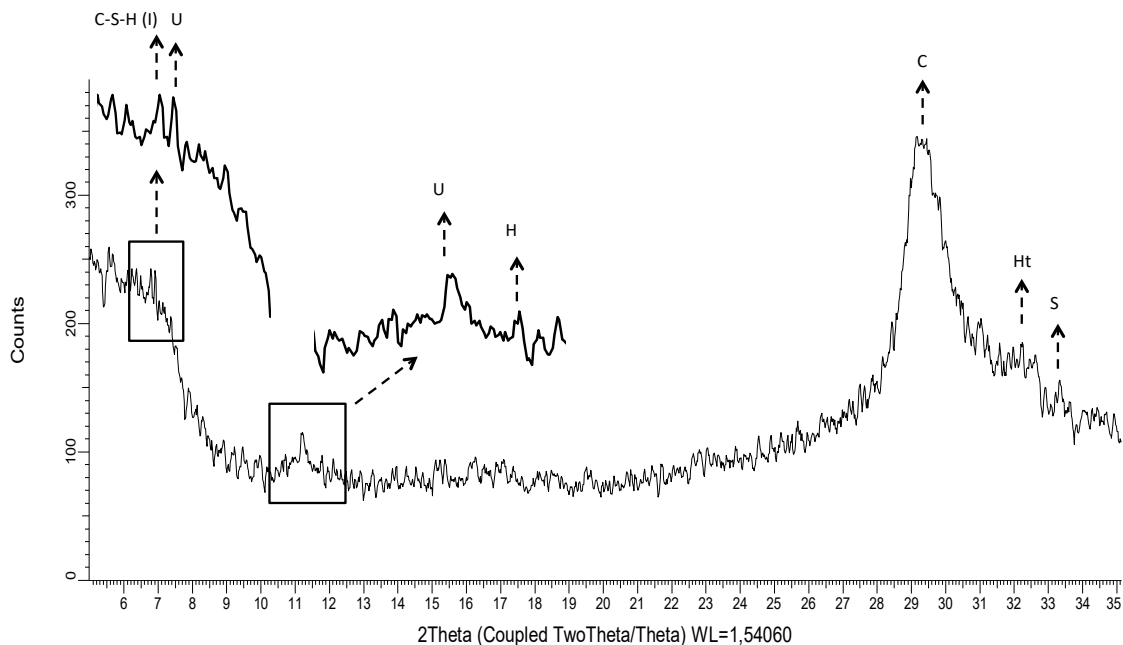
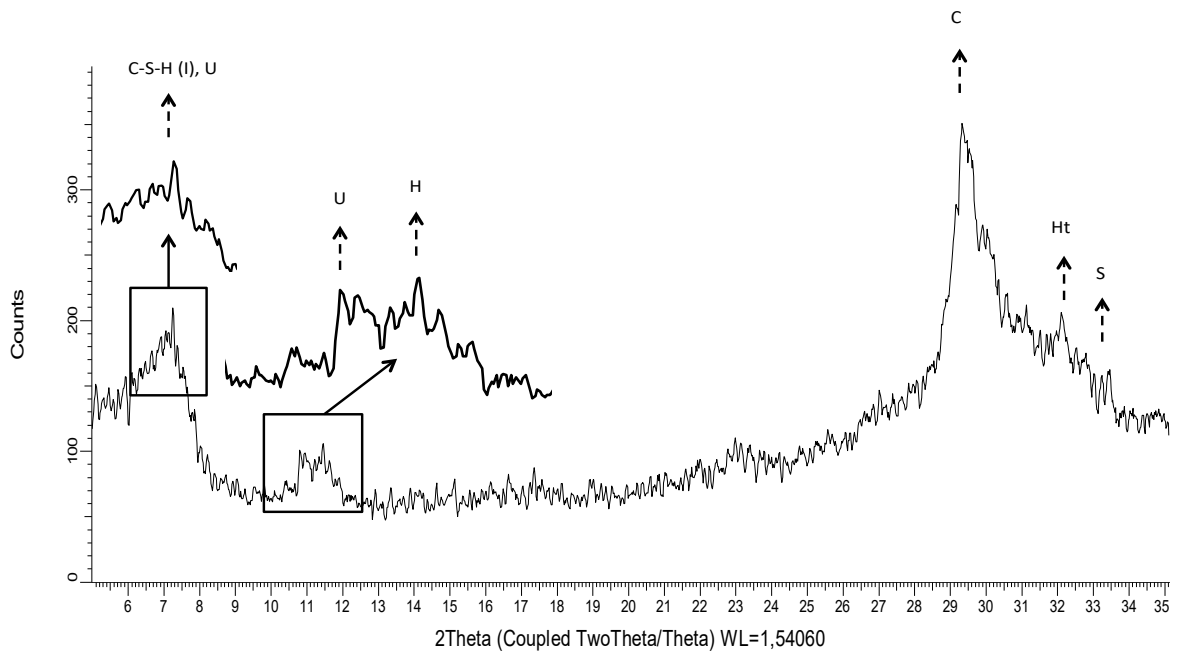
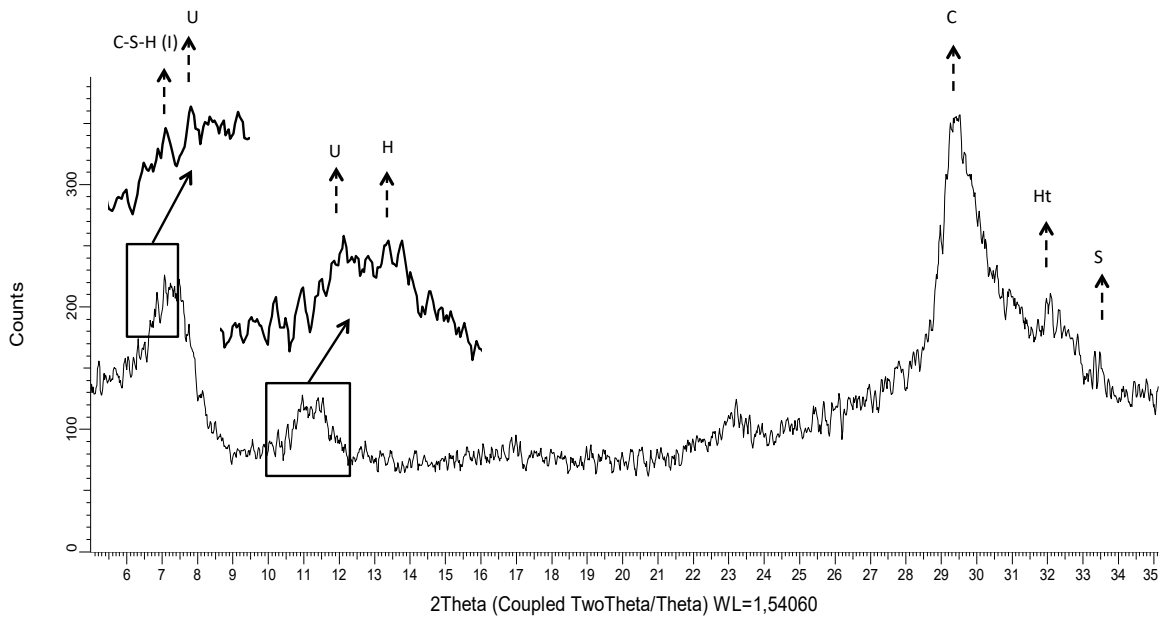


Fig.8. - X-ray diffractograms of hardened sodium silicate AASC pastes (C – calcite, H – Hydrotalcite, C-S-H (I), A – Akermanite, U – Ulexite).



a)



b)

Fig.9 - X-ray diffractograms of hardened sodium hydroxide AASC pastes mixed with borate solutions 10.5 (a), 8.5 (b), (C – calcite, H – Hydrotalcite, C-S-H (I), A – Akermanite, U – Ulexite)

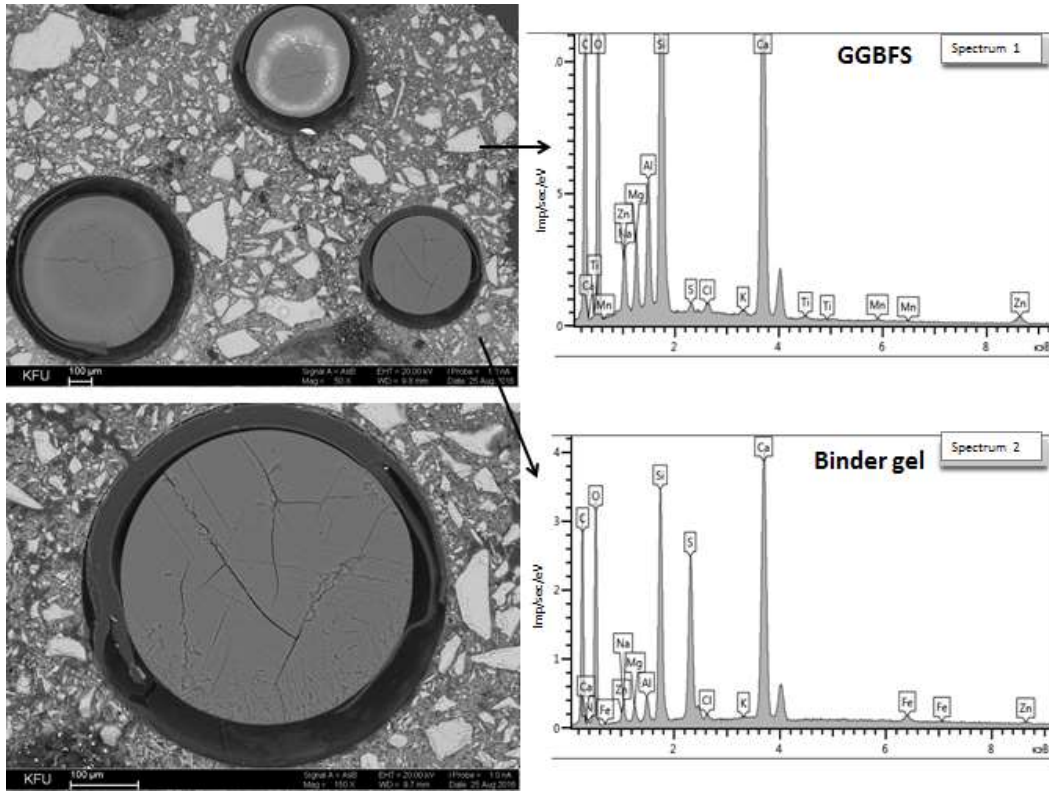


Fig. 10 - SEM image and EDS results for a hardened AASC paste that contains 30% borate-saturated IERs at a pH of 8.5.

3.3.2. Scanning electron microscopy (SEM) and energy dispersive spectroscopy (EDS)

Figure 10 shows a SEM image and EDS spectra for hardened AASC paste that contains 30% borate-saturated IERs at a pH of 8.5. Figures 11 and 12 show optical microscopy images of the same paste. The AASC waste forms exhibit a reasonably uniform distribution of IERs in the mineral matrix.

4. Discussion

Figure 4 shows the retarding effect of the borate IERs on the AASC waste sample structure formation process. It is supposed the following phenomena that causes retardation: (i) H^+ cations from the borate solution react with OH^- groups from the alkali component that are essential for activation of GGBFS and H_2O formation, and (ii) soluble $NaB(OH)_4 \cdot 2H_2O$ can precipitate on the GGBFS particle surfaces, slowing rupture of Si-O-Si bonds in GGBFS by OH^- groups. In later stages, soluble $NaB(OH)_4 \cdot 2H_2O$ reacts with Ca^{2+} to form less soluble reaction products like ulexite ($NaCaB_5O_6(OH)_6(H_2O)_5$). This product was found in the (GGBFS)-sodium metasilicate (hydroxide)-borate solution. Thus, the AASC-based mineral matrix chemically binds borate salts into insoluble ulexite.

Figures 5-7 and Table 2 show that the ability of AASC paste to maintain its strength after solidification of borate IERs is mostly determined by the nature of the alkali components. It also depends

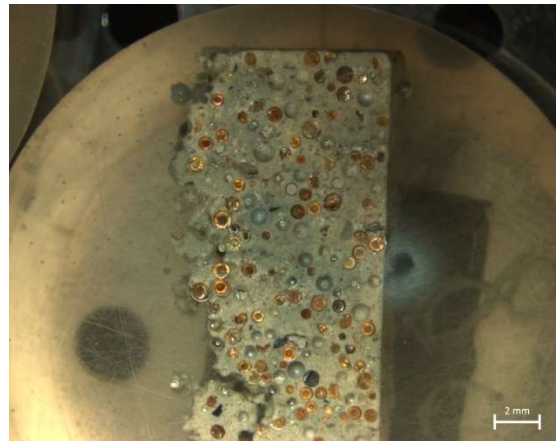


Fig. 11 - Optical microscopy of a hardened AASC paste that contains 30% borate-saturated IERs at a pH of 8.5.

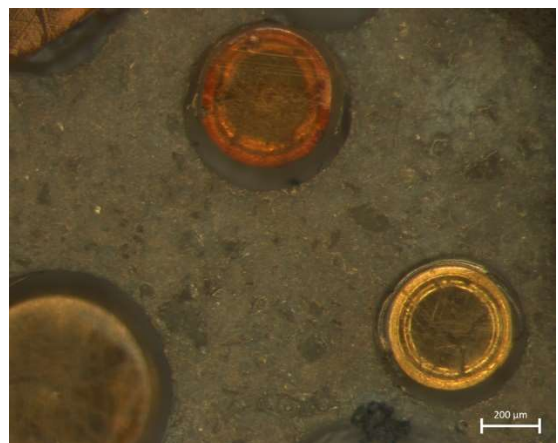


Fig. 12 - Optical microscopy of a hardened AASC paste that contains 30% borate-saturated IERs at a pH of 8.5.

on the pH of the borate solution, which influences the GGBFS hydration rate and can be increased via Na_2O concentration. The retarding effect of borate IERs is lower when they are introduced into the stronger sodium metasilicate mineral matrix than when sodium hydroxide AASC paste is used. In addition, at least 7% Na_2O must be included to produce high strength AASC pastes with up to 35% borate IERs at pH 8.5 –10.5. The borate IERs solidified using appropriate AASC-based compositions exhibit high compressive strengths and are evenly distributed in the mineral matrix.

5. Conclusions

1. The AASC-based mineral matrix was found to be suitable for solidification of borate IERs at pH 8.5–10.5. A borate IER content of up to 35% can be achieved in a sodium silicate AASC mineral matrix, resulting in 28-day compressive strengths of up to 4.7-7.3 MPa.

2. The four experimental factors showed that the ability of the mineral matrix to maintain its strength after solidification of borate IERs increases when sodium metasilicate is the alkali component, a higher Na_2O concentration is used, the borate solution pH is higher, or polypropylene fibre is introduced.

3. The main reaction products of (GGBFS)-(sodium metasilicate, sodium hydroxide)-(borate solution) systems are C-(A)-S-H, calcite (CaCO_3), hydrotalcite ($\text{MgO}_{6.667}\text{Al}_{0.333}(\text{OH})_2(\text{CO}_3)_{0.167}(\text{H}_2\text{O})_{0.5}$), calcium silicate hydrate C-S-H (I) - $\text{CaO}\text{SiO}_2\text{H}_2\text{O}$, calcium silicate hydrate C-S-H $\text{Ca}_{1.5}\text{SiO}_{3.5}\text{H}_2\text{O}$, and ulexite $\text{NaCaB}_5\text{O}_6(\text{OH})_6(\text{H}_2\text{O})_5$.

REFERENCES

1. E. Lafond, C. Cau Dit Coumes, S. Gauffinet, D. Chartier, P. Le Bescop, L. Stefan, A. Nonat, Investigation of the swelling behavior of cationic exchange resins saturated with Na^+ ions in a C_3S paste. *Cem Conc Res* 2015, **69**, 61.
2. J. Wang, Z. Wan, Treatment and disposal of spent radioactive ion-exchange resins produced in the nuclear industry. *Prog Nucl Energy* 2015, **78**, 47.
3. M. Natsuda, T. Nishi, Solidification of ion exchange resins using new cementitious material. (1) Swelling pressure of ion exchange resin. *J Nucl Sci Technol* 1991, **29**, 883.
4. P. Le Bescop, P. Bouniol, M. Jorda, Immobilization in cement of ion exchange resins. *Mater Res Soc Symp Proc* 1990, **176**, 183.
5. IAEA, 2002. Application of ion exchange processes for the treatment of radioactive waste and management of spent ion exchangers. TRS No. 408.
6. Y.Z. Zhou, G.C. Yun, Solidification of spent ion exchange resin using ASC cement. *J Tsinghua Univ Sci Technol* 2002, **7**, 636.
7. J. Li, J. Wang, Advances in cement solidification technology for waste radioactive ion exchange resins: A review. *J Hazard Mater* 2006, **B135**, 443.
8. V.N. Epimahov, M.S. Olejnik, Radioactive Ion Exchange Resin Inclusion Into Inorganic Binder. *Atom Energy* 2005, **99**(3), 171.
9. L.W. Pan, B.D. Chang, Optimization for solidification of low-level-radioactive resin using Taguchi analysis, *Waste Manag* 2001, **21**, 767.
10. M.S. Olejnik, V.N. Epimahov, V.V. Trofimov, Inclusion of radioactive ion-exchange resins into slag binder. *Radiochem* 2010, **52**(6), 516.
11. Q. Sun, J. Li, J. Wang, Solidification of borate radioactive resins using sulfoaluminate cement blending with zeolite. *Nucl Eng Des* 2011, **241**, 5308.
12. P. Kryvenko, H. Cao, P. Petropavlovskiy, L. Weng, O. Kovalchuk, Applicability of alkali-activated cement for immobilization of low-level radioactive waste in ion-exchange resins. *East-Eur J Enterpr Techn* 2015, **1/6**(79), 40.
13. N. Rakhimova, R. Rakhimov, V. Morozov, L. Potapova, Y. Osin, Mechanism of solidification of simulated borate liquid wastes with sodium silicate activated slag cements. *J Clean Prod* 2017, **149**, 60.
14. E. Shinkevich, Y. Zaytsev, Structural Durability, Deformation Properties and Fracture Mechanics Parameters of Advanced Silicate Materials, Proceeding of 18th European Conference on Fracture of Materials and Structures from Micro to Macro Scale, Dresden, Germany, 2010.
15. Y. Lutskin, E. Shinkevich, Analysis of the Relationship Between Microstructure and Properties of Activated Lime-Silica Composites on the Basis of Experimentally-statistical Modelling. *Techn J* 2015, **9**, 27.
16. Y. Lutskin, E. Shinkevich, Y. Mariyanko, Aerated Complex Activated Composites on Silicate Matrix of Thermal-moisture Hardening, Proceeding of 14th International Congress on the Chemistry of Cement, Beijing, China, 2015, 632.
17. R.O. Abdel Rahman, R.Z. Rakhimov, N.R. Rakhimova, M.I. Ojovan, *Cementitious Materials for Nuclear Waste Immobilization*. Chichester: Wiley; 2015.
